906 *Chem. Mater.* **2010,** *22,* 906–913
DOI:10.1021/cm901723j

CHEMISTRY OF MATERIALS
Article

First Principles Investigation of Oxygen Vacancies in Columbite MNb_2O_6 (M = Mn, Fe, Co, Ni, Cu)†

M. E. Arroyo y de Dompablo,*,‡ Yueh-Lin Lee,§ and D. Morgan§,∥

‡*Departamento de Química Inorgánica, Universidad Complutense de Madrid, 28040 Madrid, Spain,* §*Materials Science Program and* ∥*Department of Materials Science and Engineering, University of Wisconsin-Madison, Madison, Wisconsin 53706-1595*

Received June 22, 2009. Revised Manuscript Received September 5, 2009

This work presents a computational study on the stability and electronic properties of oxygen vacancies in candidate mixed electronic−ionic conducting columbites, MNb_2O_6 (M = Mn, Fe, Co, Ni, Cu). Calculations are based on density functional theory with the DFT+U method. Three distinct oxygen vacancy types are investigated, differing by the coordination of the oxygen atoms removed: oxygen atoms coordinated by three, two, or one Nb ion. Calculation shows that the energy of oxygen vacancy formation depends on the transition metal ion, with values ranging from 6 eV in $MnNb_2O_6$ to 3.5 eV in $CuNb_2O_6$ (data refers to one oxygen vacancy per four formula units, or 4.16% vacancies). For a given transition metal the location of the vacancy formation energies on the different sites vary by a maximum range of 0.85 eV. In both $MnNb_2O_6$ and $CuNb_2O_6$ the oxygen vacancy formation induces (a) a narrowing of the band gap and (b) an electronic density redistribution leading to the reduction of cations to lower oxidation states. For $MnNb_2O_6$ reduction affects mostly Nb^{5+} ions, while for $CuNb_2O_6$ the Cu^{2+} ions are reduced to Cu^{1+}. The potential improvement of electronic conductivity in $CuNb_2O_{6-x}$ together with the moderate vacancy formation energy makes this material a potential mixed electronic−ionic conductor.

Introduction

The electrical properties of columbite $MnNb_2O_6$ have been recently explored exprimentally[1,2] with the aim of inducing mixed ionic−electronic conductivity in this material. Given the insulating character of $MnNb_2O_6$, some alterations to the materials are required to meet this goal. One approach is to realize mixed conductivity might be creating reduced $MnNb_2O_{6-x}$, provided that the material can hold a substantial amount of anionic vacancies accompanied by an enhanced electronic conductivity. García-Alvarado et al.[1] reported the preparation of reduced $MnNb_2O_{6-x}$ ($x = 0.02$) with an improved conductivity of four orders of magnitude with respect to that of the parent columbite. However, the creation of a substantial amount of oxygen vacancies to allow good oxygen transport was not accomplished. Later attempts to create oxygen vacancies in the Ti-doped analogues were also unsuccessful.[2] The columbite structure is stable for other divalent transition metal ions such as Co, Fe, or Cu (M in MNb_2O_6),[3−6] creating the possibility of tuning the oxygen mobility/electronic conductivity by choosing a particular M ion or a combination of them. In this work the heat (enthalpy) of oxygen vacancy formation, that is, the amount of heat absorbed during oxygen release, has been calculated using density functional theory for the columbites MNb_2O_6 (M = Mn, Fe, Ni, Co, and Cu) to assess which M cation might provide the greatest opportunity for creating anion vacancies. First principles calculations also provide detailed information on the electronic structure of the materials, giving insight into the effect that oxygen vacancies will have on the electronic conductivity of columbites.

The columbite crystal structure[3] (see Figure 1) consists of layers of slightly distorted hexagonal-closed-packed oxygen octahedra perpendicular to the *a*-axis. Within each *b*−*c* layer, octahedra filled with cations are aligned in zigzag chains running along the *c*-axis with common edges. Along the *a*-axis the cations within the octahedra alternate in the sequence M−Nb−Nb−M−Nb−Nb−M. The primitive unit cell of the columbite MNb_2O_6 (M = Mn, Fe, Co, Ni, Cu) contains four formula units; therefore, for the sake of simplicity, we will refer to the $M_4Nb_8O_{24}$ formula used in the computation. To simulate a reduced form of $M_4Nb_8O_{24}$ oxygen atoms have to be removed from the structure. As shown in Figure 1, three different oxygen sites exist in the columbite structure;[3]

†Accepted as part of the 2010 "Materials Chemistry of Energy Conversion Special Issue".

*Corresponding author. Tel.: +34 91 3945222. Fax: +34 914352. E-mail: e.arroyo@quim.ucm.es.

(1) García-Alvarado, F.; Orera, A.; Canales-Vazquez, J.; Irvine, J. T. S. *Chem. Mater.* **2006**, *18*(16), 3827–3834.
(2) Orera, A.; García-Alvarado, F.; Irvine, J. T. S. *Chem. Mater.* **2007**, *19*, 2310–2315.
(3) Weitzel, H. *Z. Kristallographie, Kristallgeometrie, Kristallphysik, Kristallchemie* **1976**, *144*, 238.
(4) Norwig, J. W. H.; Paulus, H.; Lautenschlaeger, G.; Rodriguez-Carvajal, J.; Fuess, H. *J. Solid State Chem.* **1995**, *115*, 476.
(5) Wichmann, R.; Mueller-Buschbaum, H. *Z. Anorg. Allg. Chem.* **1983**, *503*, 101–105.
(6) Tealdi, C.; Mozzati, M. C.; Malavasi, L.; Ciabattoni, T.; Amantea, R.; Azzoni, C. B. *Phys. Chem. Chem. Phys.* **2004**, *6*, 4056–4061.

 Published on Web 10/02/2009

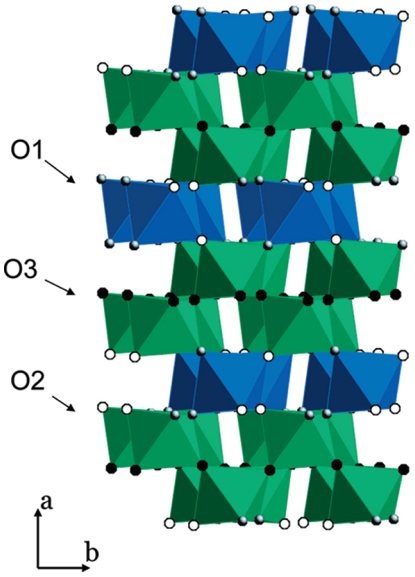

Figure 1. The crystal structure of columbite MNb_2O_6. The different oxygen sites are indicated by gray (O1), black (O2), and white (O3) balls.

O1 belonging to two Nb and one M octahedra (gray balls), O2 belonging to one Nb and two M octahedral (white balls), and O3 shared between three Nb octahedral (black balls). In this work we have selectively removed the three distinct oxygen ions to identify the most stable sublattice for oxygen vacancy formation and investigate the impact of the oxygen vacancy location in the electronic structure and stability of $M_4Nb_8O_{23}$ reduced compounds. Although the high level of oxygen vacancies in the computed cell ($M_4Nb_8O_{23} = MNb_2O_{5.75}$) is larger than we expect to be accessible experimentally, these calculations are useful to evaluate the dependence on M and oxygen site of both the vacancy formation energy and the charge density redistribution upon reduction.

Methodology

The calculations have been performed using the ab initio total-energy and molecular dynamics program VASP (Vienna ab initio simulation program) developed at the Universität Wien.[7,8] Total energy calculations based on density functional theory (DFT) were performed within the general gradient approximation (GGA), with the exchange and correlation functional form developed by Perdew, Burke, and Ernzerhof (PBE).[9] The interaction of core electrons with the nuclei is described by the projector augmented wave (PAW) method.[10] The energy cut off for the plane wave basis set was kept fixed at a constant value of 500 eV throughout the calculations. The integration in the Brillouin zone is done on a set of k-points ($2 \times 4 \times 4$) determined by the Monkhorts-Pack scheme. A convergence of the total energy close to 10 meV per formula unit is achieved with such parameters. Convergence of the band gap values extracted from the calculated DOS was confirmed using k-point grids of $3 \times 6 \times 6$ and $4 \times 8 \times 8$. The initial cell parameters and atomic positions of MNb_2O_6 were taken from Weitzel,[3] with the unit cell containing four formula units ($M_4Nb_8O_{24}$). Oxygen ions (O1, O2, or O3) were selectively removed to model the reduced forms $M_4Nb_8O_{23}$ ($MNb_2O_{5.75}$, or a 4.16% concentration of oxygen vacancies). All stoichiometric and reduced structures were fully relaxed (atomic positions, cell parameters, and volume). Spin polarized calculations were performed in all cases. Columbites are complex antiferromagnetic materials.[4,6,11] In oxides, differences among calculated total energy for distinct magnetic configurations are typically below 250 meV/(metal cation) (e.g., see refs 12 and 13). These energy differences are small compared to oxygen vacancy formation energies, which rank on the order of 2−7 eV.[14] Thus, for shake of simplicity, in this work all the columbites were initially considered in a ferromagnetic configuration, and no magnetic constrains were imposed during the relaxation. The final energies of the optimized geometries were recalculated so as to correct the changes in the basis set of wave functions during relaxation. Convergence with respect to cell size was checked by performing select additional calculations for M = Mn, Ni, and Cu on $M_8Nb_{16}O_{47}$ cells ($MNb_2O_{5.875}$ or 2.08% vacancies), and the results of these calculations are discussed below.

The overestimation of electron delocalization and metallic character is a known failure of DFT methods, in particular for systems with localized d-electrons and f-electrons.[15−17] DFT+U methods have been shown to improve the accuracy of traditional local density and generalized gradient approximation (LDA and GGA) energies for transition metal oxides.[18] DFT+U should therefore give a better description of oxygen defects in systems such as columbites, and the total energy of the optimized columbites have been calculated using the GGA+U method, following the simplified rotationally invariant form of Dudarev et al.[19] The GGA+U method combines the high efficiency of GGA and an explicit treatment of correlation with a Hubbard-like model for a subset of states in the system. Noninteger or double occupations of these states is penalized by the introduction of two additional interaction terms, namely, the one-site Coulomb interaction term U and the exchange interaction term J, by means of an effective parameter $U_{eff} = U - J$. Effective U values ($J = 1$ eV) for the d orbitals of M ions were taken from ref 18; 6.4 eV for Ni, 3.3 eV for Co, and 4 eV for Mn, Fe, and Cu. The U_{eff} value for Nb has been chosen so as to reproduce the experimental band gap of the unreduced $NiNb_2O_6$, which is reported to be 2.2 eV.[20] Test calculations for $NiNb_2O_6$ were performed using the Gaussian smearing method with a fix value of Ni-U_{eff} = 6.4 eV and varying Nb-U_{eff} between 0 and 3 eV. The calculated band gap for $NiNb_2O_6$ with Nb-U_{eff} = 0 eV is 0.93 eV and increases to 2.02, 2.21, 2.45, and 2.57 eV for Nb-U_{eff} values of 0, 0.5, 2, and 3 eV, respectively. On the basis of these initial test results a value of Nb-U_{eff} = 0.5 eV gave a correct band gap for $NiNb_2O_6$, and hence the Nb-U_{eff} was set to 0.5 eV

(7) Kresse, G.; Furthmuller, J. *Phys. Rev. B* **1996**, *54*, 169.
(8) Kresse, G.; Joubert, D. *Phys. Rev. B* **1999**, *59*, 1758.
(9) Perdew, J. P.; Burke, K.; Ernzerhof, M. *Phys. Rev. Lett.* **1996**, *77*(18), 3865–3868.
(10) Bloch, P. E. *Phys. Rev. B* **1994**, *50*, 17953.
(11) Weitzel, H.; Ehrenberg, H.; Heid, C.; Fuess, H.; Burlet, P. *Phys. Rev. B* **2000**, *62*(18), 12146–12155.
(12) Biskup, N.; Martínez, J. L.; Arroyo y de Dompablo, M. E.; Díaz-Carrasco, P.; Morales, J. *J. Appl. Phys.* **2006**, *100*, 093908.
(13) Morgan, D.; Wang, B.; Ceder, G.; van de Walle, A. *Phys. Rev. B* **2003**, *67*, 134404.
(14) Ganduglia-Pirovano, M. V.; Hofmann, A.; Sauer, J. *Surf. Sci. Rep.* **2007**, *62*, 219.
(15) Anisimov, V. I.; Zaanen, J.; Andersen, O. K. *Phys. Rev. B* **1991**, *44*(3), 943–954.
(16) Zhou, F.; Marianetti, C. A.; Cococcioni, M.; Morgan, D.; Ceder, G. *Phys. Rev. B* **2004**, *69*, 20.
(17) Ganduglia-Pirovano, M. V.; Hofmann, A.; Sauer, J. *Surf. Sci. Rep.* **2007**, *62*, 219.
(18) Wang, L.; Maxisch, T.; Ceder, G. *Phys. Rev. B* **2006**, *73*(19), 195107.
(19) Dudarev, S. L.; Botton, G. A.; Savrasov, S. Y.; J. Humphreys, C. J.; Sutton, A. P. *Phys. Rev. B* **1998**, *57*, 1505.
(20) Yea, J.; Zoub, Z.; Matsushitaa, A. *Int. J. Hydrogen Energy* **2003**, *28*, 651–655.

Table 1. Experimental and Calculated Lattice Parameters of MNb_2O_6 Columbites

lattice parameters		Mn [6]	Fe[3]	Co[3]	Ni[5]	Cu[24]
calculated	*a* (Å)	14.647	14.389	14.277	14.191	14.313
	b (Å)	5.891	5.819	5.798	5.761	5.685
	c (Å)	5.153	5.080	5.081	5.079	5.237
	V (Å^3)	444.58	425.40	420.644	415.28	426.15
experimental	*a* (Å)	14.4376(3)	14.2448(8)	14.1475(18)	14.032	14.1038(2)
	b (Å)	5.7665(1)	5.7276(5)	5.7120(7)	5.687	5.60728(8)
	c (Å)	5.0841(1)	5.0421(4)	5.0446(6)	5.033	5.12375(8)
	V (Å^3)	423.27	411.38	407.66	401.63	405.21
volume error (%)		5.0	3.4	3.2	3.4	5.2

Table 2. Calculated M−O Bond Lengths (Å) of $M_4Nb_8O_{24}$ Compounds[a]

	$M_4Nb_8O_{24}$									
bond	Mn[6]		Fe[3]		Co[3]		Ni[5]		Cu[24]	
M-O	2.179	(2.1200)	2.082	(2.0899)	2.050	(2.0422)	2.036	(2.0422)	1.957	(1.9880)
	2.180	(2.1200)	2.083	(2.0899)	2.050	(2.0422)	2.036	(2.0422)	1.957	(1.9880)
	2.181	(2.1864)	2.109	(2.1201)	2.076	(2.1219)	2.052	(2.0721)	1.992	(2.0025)
	2.183	(2.1864)	2.111	(2.1201)	2.076	(2.1219)	2.052	(2.0721)	1.992	(2.0025)
	2.226	(2.2326)	2.120	(2.1251)	2.123	(2.1463)	2.099	(2.0762)	2.523	(2.4126)
	2.231	(2.2326)	2.122	(2.1251)	2.123	(2.1463)	2.099	(2.0762)	2.523	(2.4126)
average	2.197	2.179	2.105	2.1117	2.083	2.1034	2.062	2.0635	2.157	2.1344

[a] Experimental data are given in parentheses.

for all the MNb_2O_6 and their reduced compounds. Additional later calculations of the band gap of $NiNb_2O_6$ (Nb-U_{eff} = 0.5 eV, Ni-U_{eff} = 6.4 eV) with the tetrahedron method with Blöchl corrections gave a somewhat larger value of 2.82 eV. The tetrahedron smearing method was employed for all the DOS presented in this work.

Results and Discussion

Table 1 compares the experimental lattice parameters of MNb_2O_6 (M = Mn, Fe, Co, Ni, Cu) with the computed ones. Selected bond distances are compared in Table 2. Generally speaking there is a good agreement between calculations and experiments. For $CuNb_2O_6$ the cell volume is overestimated by 5%, which is likely due to errors in the strong Jahn−Teller activity of Cu^{2+} ions. It is well documented that for Jahn−Teller distorted ions, the calculated long M−O bonds are overpredicted within an error of 3−9% as compared to experiments.[21−23] In $CuNb_2O_6$ the calculated long Cu−O bond length is 2.523 Å, to be compared with the experimental values of 2.4126 Å[24] or 2.3851 Å.[4]

The oxygen vacancy formation in columbites is described by the reaction:

$$M_4Nb_{12}O_{24} \rightarrow M_4Nb_{12}O_{23} + \frac{1}{2}O_2 \quad (M = Mn, Fe, Co, Ni, or Cu) \qquad (1)$$

From the calculated total energies of $M_4Nb_{12}O_{24}$ and $M_4Nb_{12}O_{23}$, one can extract the energy of reaction 1:

$$E_{oxygen\ vacancy\ formation} = E_{ovf} = E(M_4Nb_{12}O_{23}) + \frac{1}{2}E(O_2) - E(M_4Nb_{12}O_{24}) \qquad (2)$$

where $E(O_2)$ is the energy of the oxygen gas. The gas reference state is taken as the total energy for the ground state of a spin-polarized optimized oxygen molecule in the gas phase, plus a correction of 1.36 eV for known errors in the O_2 energy.[18] Note that these energetics of reaction do not include the free energy contributions from the gas, which can be added in a straightforward manner, as shown in ref 25. The gas effects stabilize the oxygen vacancy by about 0.3 eV at room temperature.[25]

Figure 2a shows the calculated energy of oxygen vacancy formation for the investigated cations M, and each of the types of oxygen sites (O1 triangles, O2 circles, or O3 squares). All the reaction enthalpies are positive and hence the reduction of columbites $M_4Nb_8O_{24}$ is not thermodynamically favored at 0 K. For a large reaction enthalpy, high temperature and strongly reducing agents will be needed to create oxygen vacancies. The calculated energy of reaction 1 is between 6 and 7 eV for M = Mn, Fe, Co, and Ni but decreases to the order of 3.5 eV for $Cu_4Nb_8O_{24}$. The maximum differences in the energies of reaction 1 for the distinct oxygen sites for a given cation M range from minimum value of 0.3 eV for Ni and a maximum of 0.85 eV for Fe and Cu. The O2 site (shared by two M and one Nb) is the most favorable for the

(21) Marianetti, C. A.; Morgan, D.; Ceder, G. *Phys. Rev. B* **2001**, *63*(22), 224304–15.
(22) Arroyo y de Dompablo, M. E.; Morales, J. *J. Electrochem. Soc.* **2006**, *153*, A2098–A2102.
(23) Arroyo y de Dompablo, M. E.; Ceder, G. *Chem. Mater.* **2003**, *15*(1), 63–67.
(24) Sato, M.; Hama, Y. *J. Solis State Chem.* **1995**, *118*, 193–198.
(25) Reuter, K.; Scheffler, M. *Phys. Rev. B* **2002**, *65*, 035406.

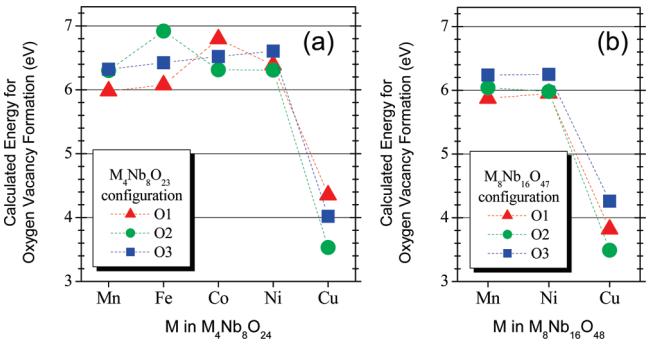

Figure 2. (a) Calculated energy of oxygen vacancy formation according to the reaction $M_4Nb_8O_{24} \rightarrow M_4Nb_8O_{23} + {}^1/_2O_2$ (M = Mn, Fe, Co, Ni, Cu). (b) Calculated energy of oxygen vacancy formation according to the reaction $M_8Nb_{16}O_{48} \rightarrow M_8Nb_{16}O_{47} + {}^1/_2O_2$ (M = Mn, Ni, Cu).

oxygen vacancy in the columbites of Co, Ni, and Cu, whereas the O1 site (shared by two Nb and one M) is the most favorable for the Mn and Fe columbites. Note that in some cases the calculated energies for the O1, O2, and O3 sites do not follow what one would expect from the number of Nb−O/M−O bonds being broken, namely, the sequence O2 (two M−O and one Nb−O)−O1 (two Nb−O and one M−O bonds)−O3 (three Nb−O bonds) For instance, in $Cu_4Nb_8O_{24}$ the energy required to create a vacancy is ordered O2 < O3 < O1. To investigate whether the trends are linked to the lattice distortions we have performed static calculations (unrelaxed) for the reduced (O1,O2,O3)−$Cu_4Nb_8O_{23}$ structures. In this case energies of oxygen vacancy formation are 4.88, 5.44, and 6.02 eV for the O2, O1, and O3 sites, respectively. Thus, the order of the vacancy formation energies vs oxygen site for Cu (O2 < O1 < O3) does seem to follow a simple bond breaking argument when relaxation is excluded. Note that the large difference between the energy of vacancy formation of relaxed and unrelaxed $Cu_4Nb_8O_{23}$ also reflects the important effect of structure relaxations.

As previously discussed for other systems,[17,26] the calculated energy of oxygen vacancy formation depends on the value of the *U* parameter utilized in the calculation. Within the pure GGA, minimum vacancy formation energy values are 5.94 and 2.71 eV for Mn and Cu, respectively (see Supporting Information Figure 1s). Comparing these energies with those of Figure 2a (GGA+U), one can conclude that the same trends in the formation energies are found with GGA as with GGA+U, with a variation in the absolute values of about 0.2 and 0.8 eV for $Mn_4Nb_8O_{24}$ and $Cu_4Nb_8O_{24}$, respectively.

A number of practical conclusions can be extracted from Figure 2a. The calculated energy of oxygen vacancy formation for $Mn_4Nb_8O_{24}$ is 5.97 eV, making it unlikely that it will be possible to induce a large amount of anionic vacancies in this material. This is consistent with experimental results; annealing $NbMn_2O_6$ at 1150 °C in 5% H_2 results in a compound $NbMn_2O_{6-x}$ with a low oxygen vacancy concentration ($x = 0.02$). For severe reducing conditions, $MnNb_2O_6$ decomposes into a mixture of

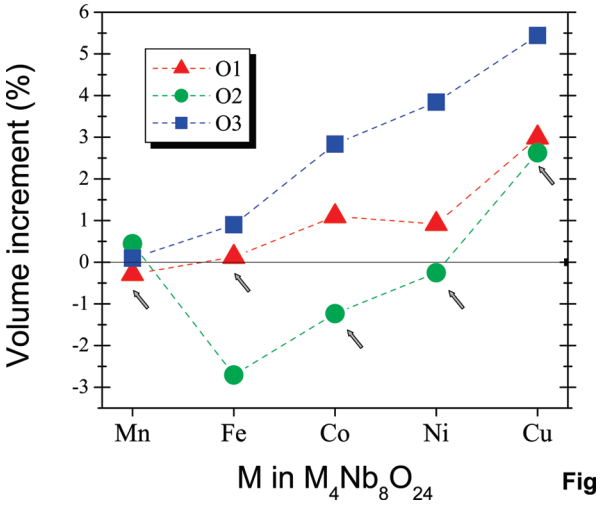

Figure 3. Calculated volume variation between $M_4Nb_8O_{24}$ and the reduced forms $M_4Nb_8O_{23}$ ($\Delta V = 100(V(M_4Nb_8O_{23}) - V(M_4Nb_8O_{24}))/V(M_4Nb_8O_{24})$). Arrows indicate the most stable form (O1, O2, or O3) for each $M_4Nb_8O_{23}$.

$MnNb_2O_{4.33}$ and $MnNb_2O_{3.67}$.[27] Oxygen vacancies are predicted to be far more easily created in $Cu_4Nb_8O_{24}$, with a minimum energy formation of 3.53 eV for the O2 site. This value is close to the vacancy energy formation calculated from first principles for materials whose reduction is feasible,[14] such as CeO_2 (2.99 eV[28]), WO_3 (2.87 eV[29]), or $FeSbO_4$ (2.81 eV[30]). Hence, $CuNb_2O_6$ is a promising material for forming a mixed electronic−ionic conductor, at least in terms of oxygen vacancy formation. So far the presented data refer to a single point defect concentration per primitive unit cell (corresponding to an oxygen vacancy concentration of 1/24 of the oxygen lattice sites, or 4.16% vacancies), which is likely larger than attainable by experiment. We have further explored the energy required to induce an oxygen defect in larger supercells of MNb_2O_6 (M = Mn, Ni, Cu). As shown in Figure 2b vacancy formation energies were found to go down (favor the vacancy formation) by a maximum of 0.4 eV for the larger system size $M_8Nb_{16}O_{47}$ ($MNb_2O_{5.875}$, or 2.08% vacancies). In some cases the order of the vacancy formation energies with respect to the O-site also changed. However, the qualitative trends identified by the smaller cell calculations were not altered and to keep the calculations practical these smaller cells will be used for the bulk of the analysis.

Figure 3 shows the calculated cell volume difference between $M_4Nb_8O_{24}$ and $M_4Nb_8O_{23}$ for the three distinct possibilities of oxygen-vacancy location (O1, O2, or O3 site). One might expect that an anionic vacancy formation would result in a cell expansion owing to the presence of both more reduced transition metal cations and oxygen vacancies. However, the volume contracts for the most

(26) Pacchioni, G. *J. Chem. Phys.* **2008**, *128*, 182505.
(27) Chumarev, V. M.; Marievich, V. P.; Pakratov, A. A. *Inorg. Mater.* **2003**, *39*(3), 352–357.
(28) Yang, Z.; Luo, G.; Lu, Z.; Hermansson, K. *J. Chem. Phys.* **2007**, *127*, 074704.
(29) Lambert-Mauriat, C.; Oison, V. *J. Phys. Condens. Matter.* **2006**, *18*, 7361–7371.
(30) Grau-Crespo, R.; Moreira, I. P. R.; Illas, F.; Leeuw, N. H.; Catlow, C. R. A. *J. Mater. Chem.* **2006**, *16*, 1943–1949.

Table 3. Calculated M−M Distances (Å) of $M_4Nb_8O_{24}$ and Its Most Stable $M_4Nb_8O_{23}$ Reduced Form

	Mn		Fe		Co		Ni		Cu	
$M_4Nb_8O_{24}$	3.301 × 2		3.129 × 2		3.073 × 2		3.073 × 2		3.262 × 2	
	O1		O1		O2		O2		O2	
	I^a	II^b	I^a	II^b	I^a	II^b	I^a	II^b	I^a	II^b
$M_4Nb_8O_{23}$	3.241	3.236	2.921	2.885	3.001	2.820	3.052	2.963	3.200	3.286
	3.330	3.296	3.201	3.201	3.066	3.176	3.075	3.108	3.234	3.360
average	3.286	3.266	3.061	2.953	3.034	2.998	3.064	3.036	3.217	3.323

[a] MO_6 polyhedron. [b] MO_5 polyhedron.

stable oxygen vacancy site of Mn, Ni, and Co. The calculated contraction of $MnNb_2O6$ (0.29%) agrees well with the experimental results of Gracia-Alvarado et al.,[1] who found a slight volume contraction of 0.22% upon reduction of $MnNb_2O_6$, which was attributed to a change in the bonding character. As shown in Table 3 the volume contraction is associated to a significant shortening of the M−M distance for the MO_5 polyhedra (the one which possesses the oxygen vacancy). This supports that the formation of oxygen vacancies in these columbites might cause a change in the bonding nature and eventually the structural degradation of the material. Indeed, it has been reported that reduction of $NiNb_2O_6$ under H_2 results in a mixture of Ni metal and NbO_2 at 600 °C.[31] For $CuNb_2O_6$ introducing an oxygen vacancy in the most stable O2 sites causes a volume expansion of 2.6%. Figure 4 shows the Cu−O and Nb−O polyhedron for the O2−$Cu_4Nb_8O_{23}$ compared to that found in $Cu_4Nb_8O_{24}$. An oxygen vacancy in the O2 sites creates two distinct M environments; two of the four M remain bonded to six oxygen ions (Cu(1) in Figure 4a), and the other two M are surrounded by five oxygen ions and the vacancy (Cu(2) and Cu(3) in Figure 4a). As seen in Figure 4a, the structural rearrangement needed to accommodate the oxygen vacancy affects mostly the CuO_5 polyhedron, and in the case of the Cu, the center labeled as Cu(3) relaxation brings the initial 5-fold coordination to a 4-fold coordination.

Figure 5 shows the calculated DOS for $M_4Nb_8O_{24}$ (M = Mn in Figure 5a and Cu in Figure 5b) and for their predicted most stable reduced $M_4Nb_8O_{23}$ compounds (M = Mn (O1 defect) in Figure 5c, Cu (O2 defect) in Figure 5d), showing the partial density of Nb ions (green) and M ions (blue). The Fermi energy is taken as the zero of energy. Both $M_4Nb_{12}O_{24}$ are semiconducting compounds with predicted band gaps of 2 eV for Mn and 1.5 eV for Cu (values within the pure GGA are 1.1 and 0.5 eV, respectively). In both columbites, the formation of an oxygen vacancy results in a narrower band gap. In $Mn_4Nb_8O_{23}$ the extra electrons from the O^{2-} fill the unoccupied Nb d states. These filled states are then at the Fermi level, and the remaining Nb d states, which used to be continuous with the now filled states, end up only slightly above the Fermi level. This creates and new band gap within the Nb d band that is narrower by 1.70 eV (reduced from 2 eV in $Mn_4Nb_{12}O_{24}$ to 0.30 eV in

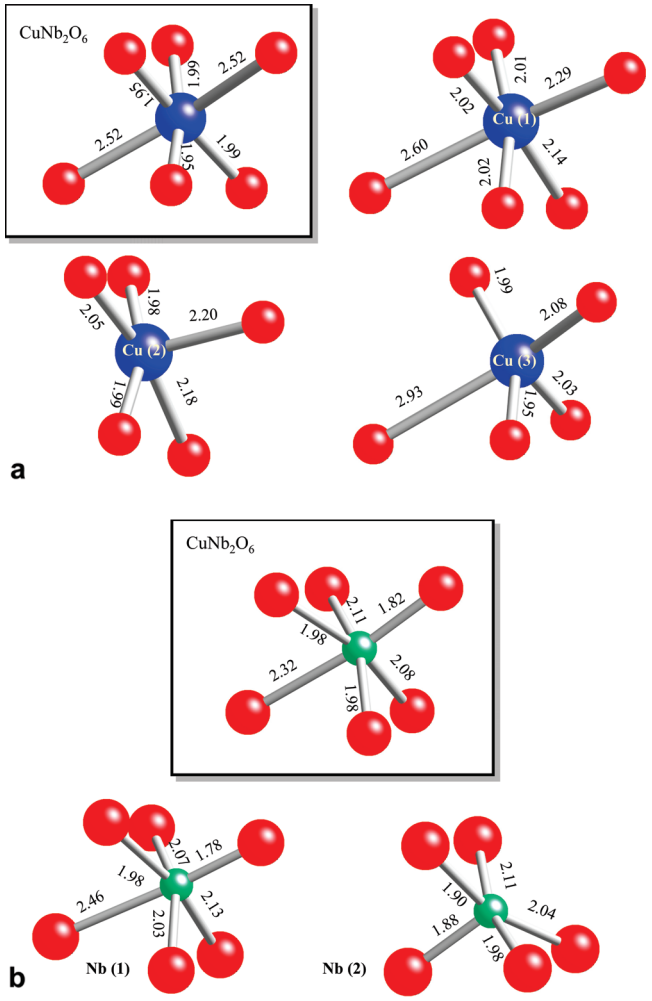

Figure 4. Coordination polyhedron of (a) the three distinct copper ions present in O2−$Cu_4Nb_8O_{23}$ and (b) the Nb polyhedra (NbO_5 and NbO_6) present in O2−$Cu_4Nb_8O_{23}$. For comparison, the insets show the cupper and niobium coordination polyhedron in $CuNb_2O_6$.

$Mn_4Nb_{12}O_{23}$). Despite the fact that $Mn_4Nb_8O_{23}$ is still a semiconductor, the small band gap (0.30 eV) in addition to a possible hopping conduction of localized electrons on the Nb (see discussion below on the nature of the metal reduction) might explain the enhanced conductivity found experimentally.[1] A similar, although less pronounced, narrowing of 0.84 eV in the band gap upon oxygen vacancy formation is found with the pure GGA approximation (the gap is reduced from 1.11 eV in $Mn_4Nb_8O_{24}$ to 0.26 eV in $Mn_4Nb_8O_{23}$). The change in DOS with vacancy formation is particularly interesting in

(31) Kunimori, K.; 0yanagi, H.; Shindo, H. *Catal. Lett.* **1993**, *21*, 283–290.

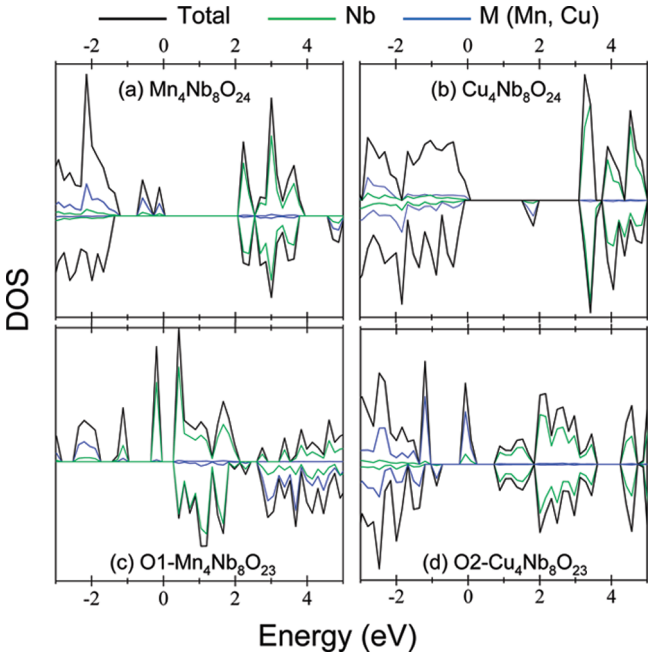

Figure 5. Calculated density of states (DOS) of (a) $Mn_4Nb_8O_{24}$, (b) $Cu_4Nb_8O_{24}$, (c) O1−$Mn_4Nb_8O_{23}$, and (c) O2−$Cu_4Nb_8O_{23}$. The black lines denote the total DOS; the partial DOS of Nb and M (M = Mn, Cu) are represented in green and blue lines, respectively. The zero of the energy has been set at the Fermi level.

$Cu_4Nb_8O_{23}$, which is predicted to be a metallic compound, though with a narrow density of states near the Fermi level. As expected, the pure GGA also predicts a metallic behavior for $Cu_4Nb_8O_{23}$. However, it is interesting to note that the band gap of the reduced columbites depends on the vacancy concentration (see Supporting Information Figure 2s). In particular, the calculated density of states of $Cu_8Nb_{16}O_{47}$ (corresponding to an oxygen vacancy concentration of 1/48 of the oxygen lattice sites, or 2.08% vacancies) shows a semiconducting behavior with a band gap of 1 eV. While the double cell is not metallic it still shows that the gap narrows significantly (from 1.5 eV in $CuNb_2O_6$) with oxygen vacancy formation. Thus, a band gap narrowing upon reduction of the Mn and Cu columbites is predicted within the GGA and the GGA+U approximation, being more pronounced in the latter. We should stress that band gap narrowing occurs in all the investigated MNb_2O_6 columbites, independently of the nature of M, location of the removed oxygen (O1, O2, or O3), or the vacancy concentration studied. The band gap narrowing contrasts with recent studies in ABO_3 perovskites[32,33] which have demonstrated that there is no band gap narrowing upon oxygen vacancy formation. One concern in the columbite studies shown here is that the reduction of the transition metals upon forming the oxygen vacancy could be an artifact of having too low a band gap, which can lead to incorrectly placing the defect state in the conduction band. However, for the one case where there is experimental data available on band gaps, $Ni_4Nb_8O_{24}$, our calculated gap (2.8 eV) is actually larger than the experimental value (2.2 eV), so there is no reason to expect that the calculated gaps are too small. More work is needed to fully understand the physics behind the band gap narrowing effect in columbites and its differences from perovskites.

As shown in Figure 5, the incorporation of an oxygen vacancy in $M_4Nb_8O_{24}$ implies the filling of the bottom of the conduction band. However, the partial DOS of M and Nb demonstrate that very different physics is associated with this conduction band filling in $Mn_4Nb_8O_{24}$ and $Cu_4Nb_8O_{24}$. In the manganoculombite (Figure 5a) the bottom of the conduction band consist on d-states from both Nb (formally Nb^{5+}) and Mn (formally Mn^{2+} with a t_2g^5 configuration) ions. In $Mn_4Nb_8O_{23}$ (Figure 5c) the top of the valence band consists mainly on Nb-d states. This indicates that Nb^{5+} ions are reduced to compensate for the oxygen vacancy formation, while Mn remains divalent. Indeed, two compounds, $MnNb_2O_{3.67}$[34] and $MnNb_2O_{4.33}$,[35] are known to contain niobium in two valence states (Nb^{2+} and Nb^{4+}) together with Mn^{2+}. In insulating $Cu_4Nb_8O_{24}$ (Figure 5b) the band right above the Fermi level is dominated by Cu d-states (Cu^{2+} configuration is $t_{2g}^6e_g^3$). This band is 1 eV lower in energy than the conduction band which is composed of the empty states of Nb^{5+}. As observed in Figure 5d, the band composed of Cu d-states gets half-filled in $Cu_4Nb_8O_{23}$. This demonstrates the reduction of Cu^{2+} to Cu^+ to accommodate the oxygen vacancy in $CuNb_2O_{6-x}$ materials. To the best of the author's knowledge there is no mixed oxide containing Nb^{4+} and Cu^{2+}, while the existence of Nb^{5+}/Cu^+ mixed oxides, such as $Cu^+Nb^{5+}{}_3O_8$[36] or $Cu^+Nb^{5+}O_3$,[37] have been reported. Furthermore, it has been shown that $CuNb_2O_6$ inserts one lithium ion at a voltage of 2.6 V vs Li due to the reduction of Cu^{2+}, while Nb^{5+} is only reduced at lower voltages, that is, at higher lithium contents.[24] These results support the hypothesis that in $Cu_4Nb_8O_{24}$ the reduction of Cu^{2+} is favored over that of Nb^{5+}.

In a first approximation, the electronic charge variation around the Cu and Nb ions due to the columbite reduction can be investigated by integrating the net electron spin density over a 2 Å radius sphere around each transition metal ion. The results are shown in Figure 6 for each oxygen vacancy location (O1, O2, or O3 site), considering the relaxed structures (left panel, Figures 6b−d) and the unrelaxed ones (right panel, Figures 6e−g). The net spin density increases steeply when integrated through the d-states of the metal ion up to 1 Å; then a plateau is observed because the charge density of the diamagnetic oxygen ions does not contribute to the spin density. The plateaus in

(32) Carrasco, J.; Illas, F.; Lopez, N.; Kotomin, E. A.; Zhukovskii, Y. F.; Evarestov, R. A.; Mastrikov, Y. A.; Piskunov, S.; Maier, J. *Phys. Rev. B* **2006**, *73*, 064106.
(33) Zhukovskii, Y. F.; Kotomin, E. A.; Evarestov, R. A.; Ellis, D. E. *Int. J. Quantum Chem.* **2007**, *107*, 2956.
(34) Burnus, R.; Koehler, J.; Simon, A. *Z. Naturforsch., B* **1987**, *42*, 536–538.
(35) Marevich, V. P.; Chumarev, V. M. *Inorganic materials* **2003**, *36*(11), 1156–1160.
(36) Marinder, B. O.; Werner, P. E.; Wahlstroem, E.; Malmros, G. *Acta Chem. Scand.* **1980**, *34*, 51–56.
(37) Marinder, B. O.; Wahlstroem, E. *Reference Chemica Scripta* **1984**, *23*, 157–160.

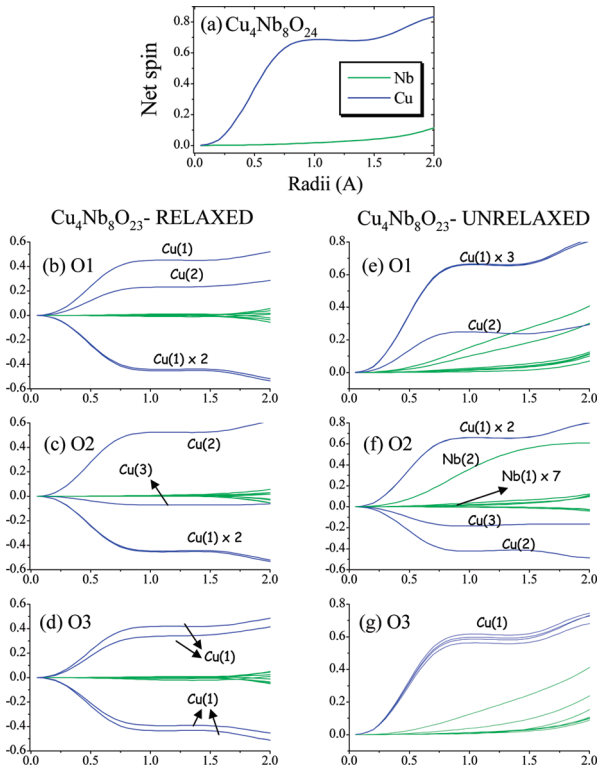

Figure 6. Integrated net spin as a function of the radius around Nb and Cu centers in (a) $Cu_4Nb_8O_{24}$ and $Cu_4Nb_8O_{23}$ for the relaxed configurations (b) O1, (c) O2, and (d) O3 and for the unrelaxed configurations (e) O1, (f) O2, and (g) O3. The distinct Cu and Nb ions in the O2−$Cu_4Nb_8O_{23}$ configuration are labeled according with Figure 4. For the other configurations Cu(1) and Cu(2) denote the sites without and with an oxygen vacancy, respectively.

$Cu_4Nb_8O_{24}$ give 0 unpaired electrons for all the eight Nb ions in the unit cell and about 0.7 spin for the four Cu ions, approaching to the spin only moments for unpaired electrons of Nb^{5+} (d^0 ion) and Cu^{2+} ($t_{2g}^6e_g^3$ configuration), respectively. As clearly observed in Figure 6b−d, in the relaxed structures, the oxygen vacancy formation induces major changes in the net spin distribution around Cu ions. Independently of the coordination of the oxygen vacancy, the common features are (a) a lower paired spin density, characteristic of the reduction of Cu^{2+} to lower oxidation states, (b) the four Cu ions per cell, which become distinct and display an antiferromagnetic configuration, and (c) only a subtle net spin change that occurs around Nb ions. Interestingly, even when the oxygen removed is coordinated by three Nb ions (O3 site, Figure 6d), the charge density redistribution affects mostly the Cu ions. This charge redistribution is obviously coupled to the aforementioned structural rearrangements around Cu due to vacancy formation. As shown in Figure 4, in O2−$Cu_4Nb_8O_{23}$ the JT distorted octahedral coordination characteristic of Cu^{2+} ions is absent in the Cu(2) and Cu(3) ions (those directly affected by the oxygen vacancy), where the distribution of distances corresponds to rather distorted polyhedra, as is not unusual

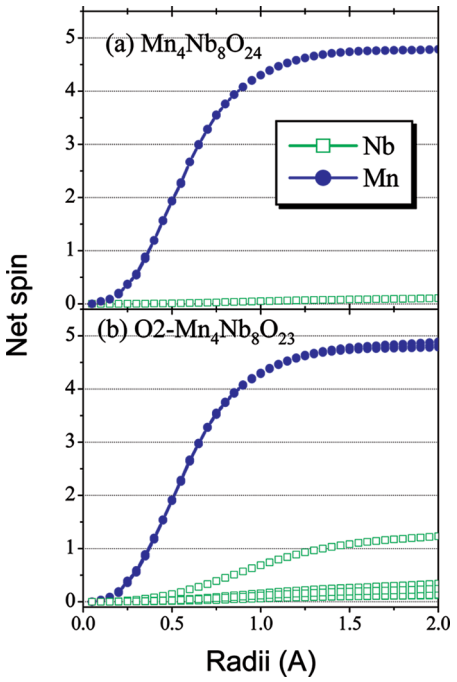

Figure 7. Integrated net spin as a function of the radius around Nb and Mn in (a) $Mn_4Nb_8O_{24}$ and (b) relaxed O2−$Mn_4Nb_8O_{23}$.

in Cu^+ compounds.[36,38−40] The loss of JT distortion on Cu(2) is consistent with their reduction from Cu^{2+} (JT active $t_{2g}^6e_g^3$ configuration) to Cu^{1+} (JT inactive $t_{2g}^6e_g^4$ configuration). To further analyze the effect of structural relaxations, spin charge densities are plotted for the unrelaxed $Cu_4Nb_8O_{23}$ configurations (Figure 6e−g). Without structural relaxation, there is a clear change in the electron density around Nb centers; in the O1 and O2 configurations both Cu and Nb ions are being reduced, and interestingly, in the O3 model there is almost no change in the electron charge around the Cu centers.

Finally, it is interesting to analyze the charge density reorganization upon reduction in the manganoculombite. As an example, Figure 7 shows the net electron spin density for O2−$Mn_4Nb_8O_{23}$, where the oxygen vacancy affects two Mn and one Nb ions, compared to that of the initial $Mn_4Nb_8O_{24}$. Introduction of oxygen vacancies in the manganoculombite clearly results in the reduction of Nb ions, whereas for the analogous configuration O2−$Cu_4Nb_8O_{23}$ (Figure 6c) only Cu ions are affected.

Conclusions

Calculation shows that the energy of oxygen vacancy formation for MNb_2O_6 (M = Mn, Fe, Co, Ni, Cu) is controlled by both the transition metal ion and the coordination of the oxygen atom that is removed. The values are about 6−7 eV for M = Mn, Co, and Ni and 3.5 eV for M = Cu (data refer to one oxygen vacancy per four formula units, or 4.16% vacancies), suggesting a qualitative difference in vacancy formation mechanism between these groups. In particular, the large difference of vacancy formation energy between $MnNb_2O_6$ and $CuNb_2O_6$ suggests that the mechanism of reduction is

(38) Krueger, T. F.; Mueller-Buschbaum, H. *Z. Anorg. Allg. Chem.* **1992**, *617*, 79–83.
(39) Rozier, P.; Satto, C.; Galy, J. *Solid State Sci.* **2000**, *2*, 595–605.
(40) Bussereau, I.; Belkhiria, M. S.; Gravereau, P.; Boireau, A.; Soubeyroux, J. L.; Olazcuaga, R.; le Flem, G. *Acta Crystallogr., C* **1992**, *48*, 1741–1744.

more complex than merely reducing Nb ions to compensate for the vacancy formation, as has been previously argued for M = Mn[1]. The electronic structure of $MnNb_2O_6$, $CuNb_2O_6$, and their reduced forms has been investigated in detail. In both $MnNb_2O_6$ and $CuNb_2O_6$ the oxygen vacancy formation induces (a) a narrowing of the band gap and (b) an electronic density redistribution leading to the reduction of cations to lower oxidation states. However, for $MnNb_2O_6$ reduction affects mostly Nb^{5+} ions, while for $CuNb_2O_6$ the Cu^{2+} ions are reduced to Cu^{1+}. The reduction of Cu^{2+} to lower oxidation states is independent of the coordination of the removed oxygen, and it is related to both the higher potential of Cu^{2+}/Cu^{+} compared to $Nb^{5+/}Nb^{4+}$ and the ease of Cu^{+} to adopt distorted polyhedra. Comparison between the charge redistribution in unrelaxed and relaxed $CuNb_2O_{6-x}$ configurations support these findings, demonstrating that Cu reduction requires structural distortions to occur. Overall, the results suggest that for the metals Mn, Fe, Co, and Ni, the introduction of vacancies reduces the Nb^{5+}, presumably due to the fact that these transition metals cannot be easily reduced below their 2+ states. However, in the case of Cu, the reduction of Cu^{2+} to Cu^{1+} greatly stabilizes the vacancy formation.

In summary, isostructural MNb_2O_6 (M = Mn, Cu) are expected to behave quite differently under reducing conditions, in terms of the stability and electronic structure of the oxygen vacancy formation. The calculations suggest that M = Cu will have improved electronic conductivity and a moderate vacancy formation energy, making $CuNb_2O_{6-x}$ a potential mixed electronic−ionic conductor.

Acknowledgment. This work was supported by Spanish Ministry of Science (MAT07-62929). Calculations were performed at the CIEMAT supercomputing centre and the NSF National Center for Supercomputing Applications (NCSA - DMR060007). Y.-.L.L. gratefully acknowledges financial support from the NSF MRSEC program (0079983). M.E.A.yD. thanks M. Lopez-Blanco, A. Orera, F. Garcia-Alvarado and U. Amador for valuable comments.

Supporting Information Available: Calculated energy of oxygen vacancy formation (GGA data) and calculated density of states of $M_8Nb_{16}O_{47}$ (M = Mn, Cu) (PDF). This material is available free of charge via the Internet at http://pubs.acs.org.